The Nucleus ***53****, No. 1 (2016) 38-48*

www.thenucleuspak.org.pk

The Nucleus

ISSN 0029-5698 (Print)

ISSN 2306-6539 (Online)

Study of Textural and Petrographic Features in Mansehra Granite, Pakistan: Implications on Gamma Radioactivity and Dose Rates

M. Anees[1*], A. A. Wajid[2], A. A. Qureshi[3], I. A. K. Jadoon[4], S. Manzoor[3], A. Atique[5] and A. Masood[4]

[1]*Department of Earth Sciences, Quaid-i-Azam University, Islamabad, Pakistan*

[2]*Oil and Gas Development Company Limited, OGDCL, Islamabad, Pakistan*

[3]*Radiation Physics Laboratory, Physics Department, COMSATS Institute of Information Technology, Islamabad, Pakistan.*

[4]*Department of Earth Sciences, COMSATS Institute of Information Technology, Abbottabad, Pakistan.*

[5]*Technische Universität Darmstadt, Darmstadt, Germany*

muhammad.anees.pk@gmail.com; aliabbaswar@gmail.com; aziz_qureshi@comsats.edu.pk

ARTICLE INFO

Article history :
Received : 18 November, 2015
Revised : 26 February, 2016
Accepted : 03 March, 2016

Keywords:
Mansehra granite,
Natural radioactivity,
Petrography,
Radioactive minerals,
Annual effective dose,
(HPGe) gamma-spectrometer,
Building material

ABSTRACT

Assessment of natural radionuclides and annual effective dose rate in Granite from Mansehra Pakistan has been carried out in this work. Overall, Mansehra Granite possess porphyritic fabric with primary minerals observed in petrography include quartz, microcline, plagioclase, biotite, muscovite etc. The study area was categorized into four zones on the basis of megascopic and microscopic features of the granite. One of the zones contained higher proportions of dark minerals like biotite, zircon, magnetite and tourmaline. This zone yielded slightly higher values of specific activities of ^{226}Ra, ^{232}Th and ^{40}K; i.e. 29.27, 51.89 and 942.66 Bq kg^{-1}respectively and annual effective dose rate of 0.96 mSv y^{-1}. When comparing with the average values of specific activities of ^{226}Ra, ^{232}Th and ^{40}K and total annual effective dose from granite from around the world it was found that overall, Mansehra granite does not pose a radiological hazard. Mansehra Granite is found to be safe and can be used as a building material. It is however, emphasized that construction of basements in the area of high activity should be avoided and granite from such areas may be used on a limited scale.

1. Introduction

Natural radiation is the major contributor towards environmental radioactivity. Naturally Occurring Radioactive Materials (NORMs) are present in earth's crust in small but quantifiable quantities. Gamma radiations emitted mainly from ^{226}Ra, ^{232}Th and ^{40}K, are the major external source of damage to living cells and tissues. ^{226}Ra, ^{232}Th and ^{40}K and their decay series which are responsible for terrestrial background radiation, exist in all earthly spheres. These radionuclides pose radiation exposure threats which can be either external due to gamma emissions or internal due to radon inhalation. These radionuclides emit alpha particles with the former (gamma) contributing 46% and latter (alpha) 54 % [1] respectively, to the total annual effective dose. Worldwide, strong measures have been taken to minimize risks of health hazards related to radiation exposure, for which limits have been set [2].

Natural radioactivity is dependent upon local geological conditions. High natural radioactivity is commonly linked with igneous rocks like granite, granodiorites and syenites, while sedimentary rocks are mostly known to be less radioactive [2]. Granites are plutonic rocks that commonly occur in large orogenic belts and continental shield areas and are usually associated with great batholiths occupying thousands of square kilometers. Minerals that contribute to the general composition of granite are; coarse grained quartz, potassium feldspar and plagioclase feldspar along with variable amounts of mica. Granites also contain radioactive minerals and can exhibit high concentrations of Uranium (1-10 ppm), Thorium (5-30 ppm) and Potassium (4% as K_2O) as compared to low abundance of these elements in the mantle and earth's crust as a whole [3, 4].

Natural radioactivity in igneous rocks depends upon their mineralogical and chemical composition [5]. Minerals can host radioactive nuclides either as basic elements or as substitute elements in their composition. K-rich minerals containing uranium and/or thorium, contribute to the high levels of natural radioactivity in rocks [5]. Igneous rocks, such as granites, are rich in U and Th bearing minerals [6]. Accessory minerals such as rutile, apatite, sphene, epidote, allanite, zircon, monazite,

* Corresponding author

thorite, uraninite, etc. have higher proportion of total uranium content in granitic rocks [7, 8]. K-rich minerals (K-feldspars, biotite) along with other accessory minerals are also contributors to the natural radioactivity in granites [9, 10].

Mansehra Granite (Cambrian) lies in the western part of the Lesser Himalayan granite belt. It is a large plutonic body which crops out in the west of the western syntaxis of the Himalayas (Fig. 1). It covers some 1800 km^2 between the Hazara-Kashmir Syntaxis (HKS) and the Indus River [11]. Mansehra granitic pluton is classified into; Susalgali gneisses, Mansehra porphyritic granites, Andalusite granites and associated minor bodies [12]. Mansehra Granite is essentially composed of alkali feldspar (30 %), quartz (30 %), plagioclase (20 %), and mica (15 %) [13].

This study, an extension of an earlier study [14], focused on the mineralogical changes in granite; textural variations inside the sampling grid and their impacts on resultant gamma radioactivity and annual effective dose rates. It is important to study radiation levels present in the building material for determining the population exposure to radiation, as Mansehra Granite is widely used as building material and decorational stone.

2. Material and Methods

2.1 Study Area, Sample Collection and Preparation

Study area consisting of the Mansehra Granitic Pluton, covering the suburban regions of Mansehra city located between 34°20'00"N to 34°21'21" N Latitude and 73°10'30" E to 73°12'10" E Longitude, was assessed for natural radioactivity using High Purity Germanium (HPGe) detector and gamma spectrometry.

Sampling grid covering an area of 2.5 × 2.5 km was adopted to collect 30 samples. Sampling was carried out in a grid pattern which was designed to cover most of the populated areas along with exposed granitic rocks (Fig. 1). Geo-morphologically, granitic rocks, in the eastern parts of the grid, were exposed in the form of distant patches and ridges where most of the area was populated, while towards the north-west of the grid, granites were emplaced as hills with villages few and far between. Samples were collected from the main granitic body. Around 5-10 cm weathered surface was removed to collect fresh sample. Sample bags, made of cotton cloth, were used for the protection and preservation of samples. Each sample weighed around 5-8 Kg. Each sample was marked according to a distinct label as shown in sampling grid (Fig. 1).

Samples were crushed using a jaw crusher and then sieved down to sand sized particles (2 mm). An electric oven was used to remove moisture and aid radon exhalation by providing temperate of 110°C for 24 hours. Net weight of samples was noted after moisture removal. Samples were sealed separately in standard 1000 ml Marinelli beakers and stored for 40 days so that radionuclides could attain secular equilibrium.

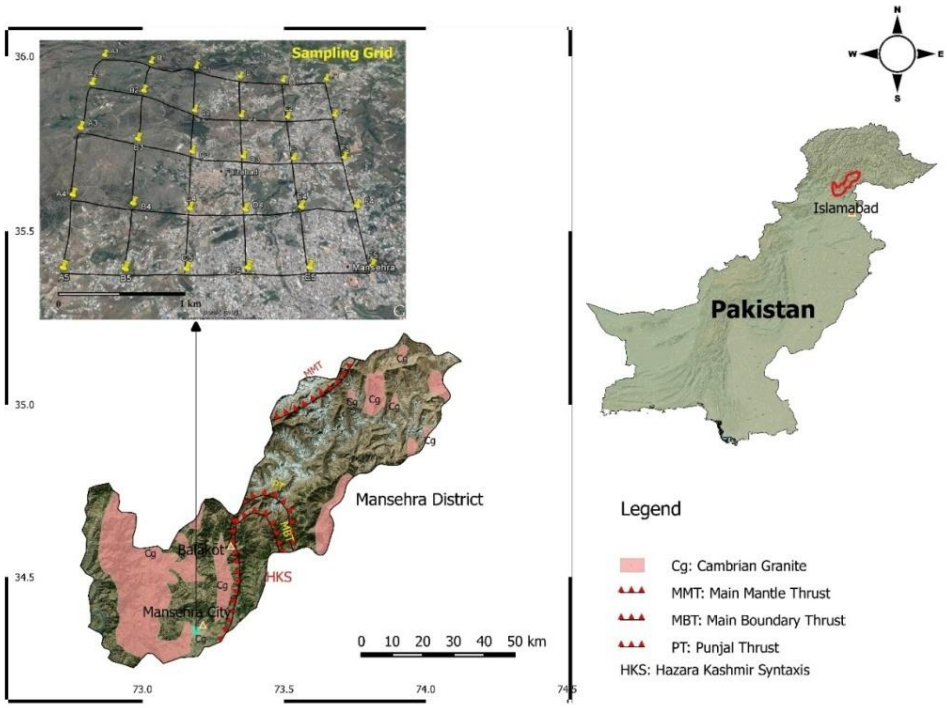

Fig. 1: Overlay of Mansehra Granite over Mansehra District [15], North Pakistan, superimposed on aerial imagery depicting zones of Cambrian Granite bodies. Regional faults (MMT= Main Mantle Thrust and MBT= Main Boundary Thrust). Study area is zoomed in to show geometry of sampling grid near Mansehra City. (Aerial Image Courtesy: Google maps and Bing maps)

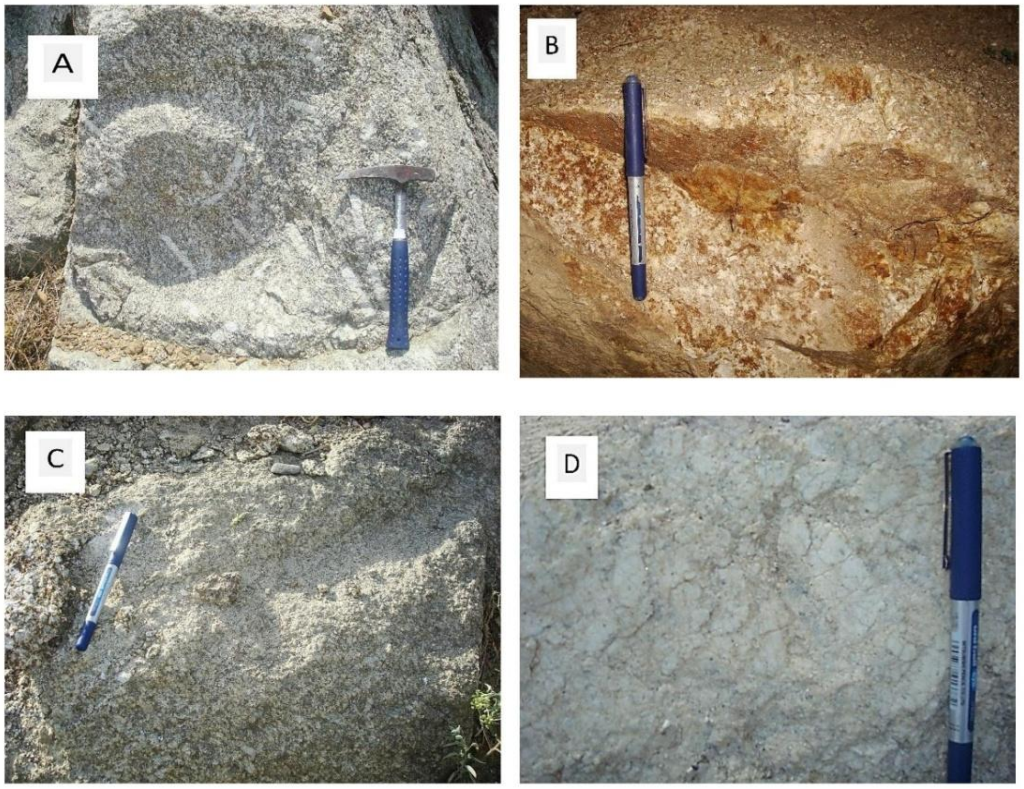

Fig. 2: Textural comparisons for major zones observed in Mansehra Granite sampling gird. (A) Zone 1 outcrop with large, white coloured phenocrysts of quartz and feldspars (B) Zone 2 outcrop embedding rusty texture, due to iron bearing micaceous minerals (C) Zone 3 outcrop depicting weathering prone granite which has undergone defragmentation of minerals. (D) Zone 4 outcrop bearing white coloured granite with high feldspar content. (*Hammer and pen for scale*)

2.2 Field Observations

Field observations were carried out in sampling grid using hand lens to study textural and visible mineralogical variations. Granitic outcrops present in the vicinity of the city boundary are whitish grey, coarse to very coarse grain and strongly porphyritic. Distinctive large phenocrysts of alkali feldspar can be easily identified. Megascopic minerals identified in field study were; quartz, plagioclase, alkali feldspar, muscovite and biotite. Representative outcrops were categorized and classified, based on megascopic textural variations (Fig. 2). Fig. 3 portrays different zones based on textural variations in Mansehra granite within the sampling grid; demarked with different coloured symbols. Major textural observations are briefly discussed and classified as follows:

2.2.1 South eastern zone 1

Mansehra Granite in South East, Zone-1 of grid, appeared as whitish grey, massive, hard and porphyritic rock with megacrysts ranging from 3 cm to 12 cm. This typical granite was strongly porphyritic with phenocrysts of alkali feldspar with coarse to very coarse grained groundmass. Biotite was prominent as brownish black flakes in hand specimen. The texture of this particular zone is shown in Fig. 2A, where visible large white coloured porphyries are embedded in matrix. This type of textural variety is marked with cyan colour as Zone 1 (Fig. 3).

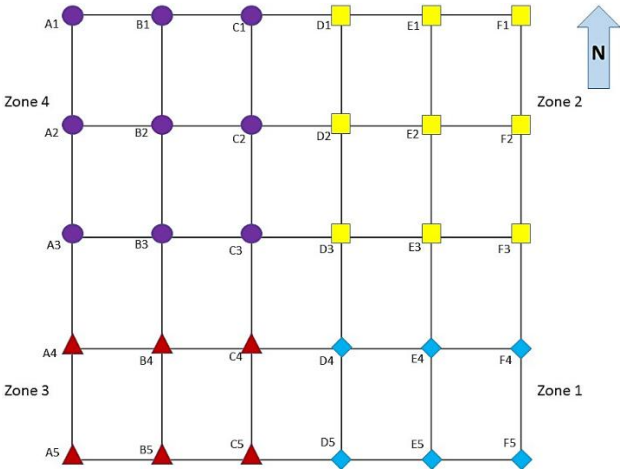

Fig. 3: Simplified graphical representation depicting textural variation zones in granite at sampling sites. Zone 1 (cyan) depicts porphyritic textures with large phenocrysts. Zone 2 (yellow) depicts rusty coloured granite marked by weathering. Zone 3 (red) shows porphyritic texture with fractures. Zone 4 (purple) shows granite with high feldspar content.

2.2.2 North eastern zone 2

Outcrops of Mansehra Granite towards northeast of sampling grid were grey to rusty grey, dirty white and coarse-grained. Prominent minerals observed in this zone were quartz, potash feldspar (orthoclase) and plagioclase with minor quantities of biotite. Feldspar was distinguished by dull white appearance whereas quartz was identified by its diagnostic vitreous lustre. Iron bearing minerals, e.g. Biotite were responsible for the rusty brown colour on weathered surface [13]. Fig. 2B shows granite with a particular rusty colour due to the presence of iron bearing minerals. Yellow coloured Zone 2 depicts this type of texture in Fig. 3.

2.2.3 South-western zone 3

Towards the south-western part of the grid, granitic outcrops were very coarse grained and porphyritic in texture, shown in red colour (Fig. 3). The granite from this area was light greyish to dull white, coarse grained with relatively high plagioclase. Reddish brown to brownish black biotite was prominent and was generally dispersed in rock and occasionally formed local aggregates. The samples from this zone, also displayed fractures and possessed similarities with the samples of Zone 1, but comparatively had more plagioclase and less quartz. The degree of weathering seemed to be greater in this zone, mainly due the presence of feldspar minerals. This effect is shown in Fig. 2C where granite has undergone weathering.

2.2.4 North western zone 4

Towards the Northwest of the sampling grid, various intrusions of feldspars as plagioclasic dikes were observed as cutting the main granitic body as a result of which original composition of granite was pretty much diluted. The milky white colour of samples from this zone depicted an increase in concentration of feldspar group of minerals. The samples from this zone were comparatively deficient in quartz and micaceous minerals. The texture of this zone is noticeable in Fig. 2D.

2.3 Petrography

Thin sections were prepared to carry out detailed petrographic study in order to confirm the megascopic observations. A thin slice (approximately 3 mm thick) was cut from the sample. This slice was then cemented on a glass slide using Canada balsam. A standard thickness of 0.03 mm was achieved by grinding the slide on a rotating lap with silicon carbide powder. Finally, the slide was polished using diamond paste to eliminate scratches. These thin sections were then studied under polarizing microscope which was connected to a computer and a digital camera.

Modal analyses were carried out using point counting method. Point counting method provided quantitative data on the relative percentage of each mineral present in a sample. Point counting was performed using image analysis software which superimposed an imaginary grid over the digital images of samples. Mineral present under each point of the grid was identified and recorded via digital camera connected to a petrographic microscope.

2.4 HPGe Gamma Ray Spectrometry

A Cobalt (^{60}Co) source from IAEA was used for energy calibration of the High Purity Germanium gamma ray spectrometer. The standard was kept in a Marinelli beaker and the standard peak was taken by measuring the sample in the detector. It was measured for 15000 seconds to get the required spectrum. For the measurements, packed dry Marinelli Beaker's samples were in high purity germanium detector (HPGe) for gamma spectrometry. The gamma-ray photo peaks corresponding to 295 keV (^{214}Pb), 351 keV (^{214}Pb), 609 keV (^{214}Bi), 1120 keV (^{214}Bi) and 1764 keV (^{214}Bi) were used for ^{226}Ra, while 238 keV (^{212}Pb), 338 keV (^{228}Ac), 463 keV (^{228}Ac), 583 keV (^{208}Tl), 911 keV (^{228}Ac), 968 keV (^{228}Ac) and 2614 keV (^{208}Te) were used for identifying ^{232}Th in the samples [16]. ^{40}K was identified from its single peak of 1.460 MeV. Counting was carried out for a time period of 15,000 seconds for each sample.

2.4.1 Specific activity calculation

Specific activity or activity concentration can be defined as the amount of radioactivity (or rate of decay) of a certain radionuclide per unit mass of that radionuclide. Specific activities of ^{226}Ra and ^{232}Th were calculated on the basis of peaks of their respective daughter products (^{214}Pb and ^{214}Bi for ^{226}Ra; ^{228}Ac and ^{208}Tl for ^{232}Th) which were in equilibrium with their parent radionuclides. Specific activity of ^{40}K is based upon its single peak at 1460.80 keV [17, 18].

The formula used to calculate specific activity for a particular radionuclide is given below;

$$A_{Ei} = \frac{N_{Ei}}{\varepsilon_E \times t \times \gamma_d \times M_s} \ (Bqkg^{-1}) \qquad (1)$$

Where; $A_{Ei=}$ Activity Concentration in Bq kg^{-1}, N_{Ei} = Net area under the peak at energy E, ε_E = Efficiency of detector at energy E, t = Counting time in seconds, γ_d = Gamma ray decay of particular radionuclide for a transition at energy E, M_s = Mass of sample in kg.

2.4.2 Dose rate calculation

The hazard levels of radionuclides in the Mansehra Granite were measured through the hazard indices that incorporate specific activity values of ^{226}Ra, ^{232}Th and ^{40}K using the formulae given in literature [14]. Annual effective doses i.e. Outdoor effective dose (E_{out}) and Indoor effective dose (E_{in}) were used as standard parameters for radiological hazard assessment of the

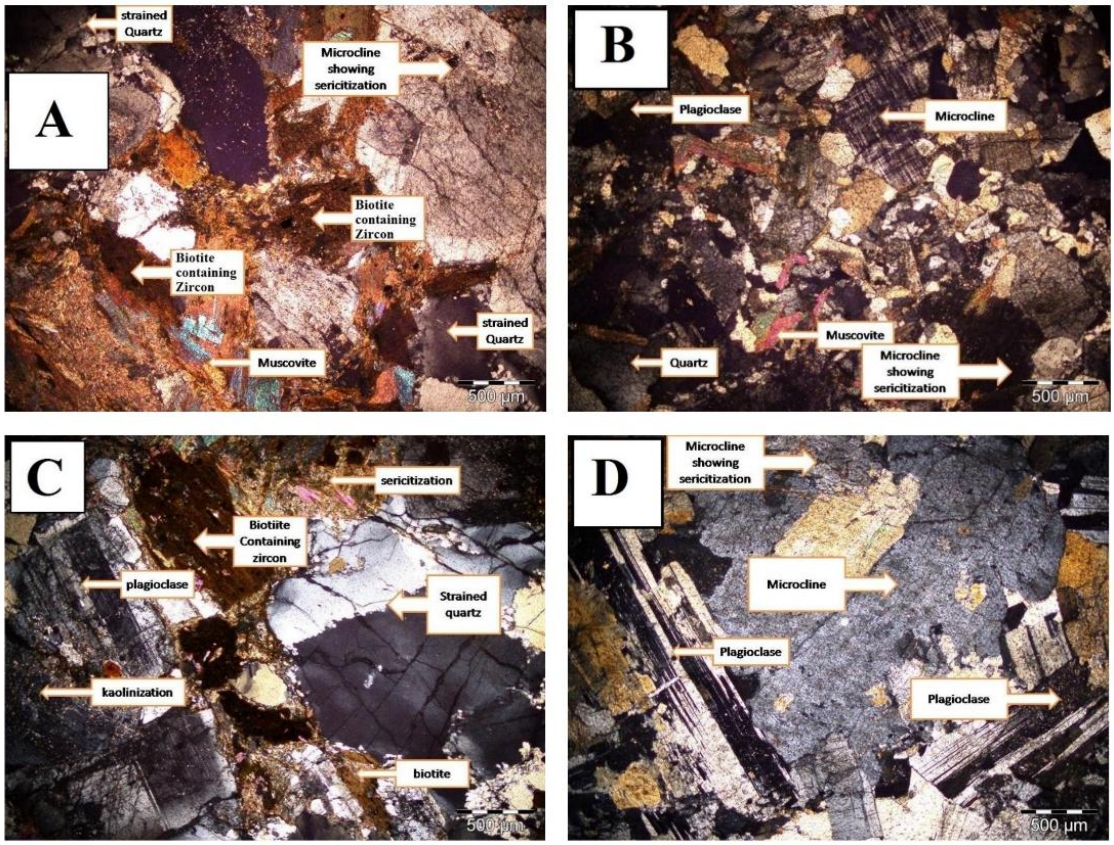

Fig. 4: Photomicrographs (PPL) of characteristic textural zones in Mansehra Granite. (A) Zone 1: Quartz, altered feldspar (microcline) along with biotite, containing inclusions of zircon (radioactive mineral) and muscovite. (B) Zone 2: Bright colours due to high birefringence of micaceous minerals along with sericitized microcline. (C) Zone 3: Weathering prone granite which has been altered (Kaolinitization and Sericitization). (D) Zone 4: Granite with high feldspar content (Plagioclase and microcline). Sericitization observed along the mineral grain work.

study area. Annual outdoor effective dose (E_{out}) was estimated from the net outdoor external (gamma) dose rate D_{out} by including time spent by an individual in the radiation area also referred to as "occupancy factor" (OF) and "conversion factor" (CF) to transform D_{out} to effective dose received by a person. Annual Outdoor Effective dose (E_{out}) is calculated using the Eq. 3 [19].

$$D_{out} = 0.462\ A_{Ra} + 0.604\ A_{Th} + 0.042\ A_K (nGy\ h^{-1}) \quad (2)$$

$$E_{out} = D_{out} \times 1.226 \times 10^{-2} (m\ Svy^{-1}) \quad (3)$$

Annual indoor effective dose (E_{in}) was calculated on the basis of occupancy factor (OF) and transforming the absorbed dose (D_{in}) in air to effective dose received by the person [20] using the conversion factor (0.7 x 10^{-6} Sv y^{-1}). Occupancy factor (OF) was taken as 0.8 (80%) so, the time spent indoors is 8760 x0.8 h y^{-1}. Therefore E_{in} can be calculated by the following equation:

$$D_{in} = 0.92\ A_{Ra} + 1.1 A_{rh} + 0.084\ A_k\ (nGy\ h^{-1}) \quad (4)$$

$$E_{in} = D_{in} \times 8766 \times 0.8 hy^{-1} \times 0.7 \times 10^{-2}\ (mSvy^{-1}) \quad (5)$$

Total Effective dose (E) was calculated by adding values of both Indoor effective dose (E_{in}) and Outdoor effective dose (E_{out}).

3. Results and Discussion

3.1 Petrographic Observations

Mansehra granite primarily comprises of microcline, quartz, plagioclase and micas (muscovite and biotite). Medium to coarse-grained Microcline (30–45 %) with euhedral phenocrysts and subhedral to anhedral ground mass show perthitic character, partly replaced by fine muscovite. Plagioclase (albite) constituted 25–40 % while Quartz (10 –25 %) was fine to medium-grained variably strained and showed wavy extinction along with small fractures. Biotite and muscovite (3–10 %) were stretched, twisted, randomly oriented, broken and curved which showed the effects of stress [21]. Alteration of feldspar minerals into clay minerals like kaolinite, chlorite and sericite were also prominent in this part of Mansehra Granite. Traces of tourmaline, magnetite, zircon, and apatite were also observed in Mansehra Granite which could be related to hydrothermal mineralization [22].

Petrographic studies were carried out for each of the four representative samples selected based on field observations from each zone, respectively (Fig. 4). Major minerals and features observed in each zone are as follows;

1. Thin section studies of Zone 1 revealed large subhedral to euhedrel medium to coarse grained crystals of microline showing sericitization along with fractured subhedral medium grained quartz and flakes biotite containing inclusions of zircon (Fig. 4A). Strained quartz which was formed as a result of hydrothermal exsolution was also observed in this sample. Results of modal analysis represent high quantity of alkali feldspar (40-45%) relative to quartz and plagioclase along micas (7-10%) and other accessory minerals (Table 1).
2. Twinned microcline, subhedral plagioclase and quartz with granular subhedral crystals were dominant in Zone 2. Biotite and muscovite were also observed with noticeable grain elongation and deformation (Fig. 4B). Sericitization was common in alkali feldspars. Modal mineralogical composition revealed slightly higher percentage of plagioclase (35-40%) while lesser percentage of alkali feldspar (30-35%) was observed as compared to Zone 1 (Table 1).
3. In Zone 3 coarse flakes of biotite, up to 1 mm, were dominant along with plagioclase, quartz, microcline and muscovite. Quartz was highly fractured while alterations were prominent along fractured margins of plagioclase and microcline. Dark black spots of inclusions of zircon were clearly identified in biotite (Fig. 4C). Kaolinite and sericite observed in feldspar minerals confirmed megascopic observations in this zone. Quartz 15-20%, Alkali feldspar 40-45%, Plagioclase 30-35% and Biotite upto 5% were principal minerals of this zone (Table 1).
4. Zone 4 was dominant in coarse grained, subhedral to euhedral plagioclase and microcline showing prominent sericitization. Mica and Quartz were observed in lesser quantities (Fig. 4D). Modal analysis showed high amounts of plagioclase 35-40% and microcline 30-35% and lesser quartz (10-15%) and mica (up to 5%) content. Minor quantities of apatite and chlorite were also observed in this zone (Table 1).

QAP triangular plot confirms megascopic observations showing distinct signature for each zone (Fig. 5). Zone 1, being dominant in alkali feldspar, is plotted towards left near alkali feldspar while Zone 4, rich in plagioclase and deficient in quartz is plotted towards lower right end. The other two Zones were plotted in between these two extremes. Petrographic observations in

Table 1: Modal Mineralogical Compositions (estimated through point counting method) of granite samples from four identified zones.

Minerals	Percentage Mineral Abundances			
	Zone 1	Zone 2	Zone 3	Zone 4
Quartz	20 – 25	20 – 25	15 – 20	10 – 15
Microcline	40 – 45	35 – 40	40 – 45	30 – 35
Plagioclase	25 – 30	30 – 35	30 – 35	35 – 40
Muscovite	4 – 5	4 – 5	2 – 3	2 – 3
Biotite	3 – 4	2 – 3	4 – 5	1 – 2
Magnetite	2 – 3	2 – 3	Trace	Trace
Tourmaline	1	1 – 2	1 – 2	1
Zircon	1 – 2	1	1 – 2	1
Chlorite	Trace	2 – 3	2 – 3	2 – 3
Apatite	Trace	Trace	Trace	1 – 2
Other Accessory minerals	2 – 3	2 – 3	2 – 3	2 – 3

Mansehra granites when compared with worldwide granites [9, 23, 24) show prominent calc-alkaline composition (Table 2). Mansehra Granite holds an intermediate position but with a slight shift toward a less silica-magnesium and high alumina domain for the same content in dark minerals [25].

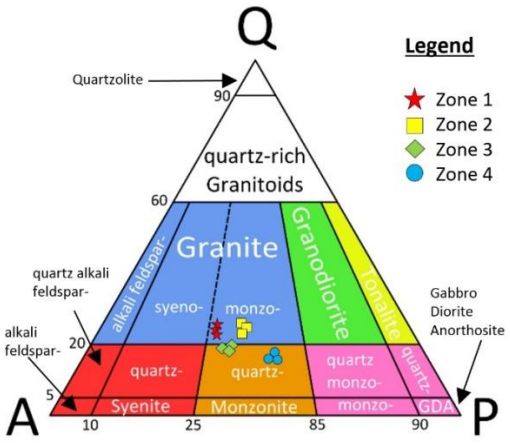

Fig. 5: QAP Plot depicting the relative proportions of Q, A and P (Q=Quartz, A=Alkali Feldspar and P=Plagioclase) in 12 thin sections from 4 pre-classified zones. Zone 1 and Zone 2 fit in Monzo-granite which contains Alkali feldspar (>35%), Quartz (>20%) and Plagioclase <50%). Zone 3 and 4 belong to Quartz Monzonite which contains Alkali feldspar (<65%), Quartz (<20%) and Plagioclase (>35%)

3.2 Specific Activity Concentration

Specific Activities of ^{226}Ra, ^{232}Th and ^{40}K in Mansehra granite vary between 17.56 to 50.91, 23.47 to 87.01 and 197.65 to 1227.82 Bq kg^{-1}, with an average of 28.88, 51.57 and 962.03 Bq kg^{-1} respectively. Activity concentration of ^{226}Ra, ^{232}Th and ^{40}K are highest in

Table 2: Petrographic correlation of Mansehra Granite with worldwide granites. Comparisons are based on texture, rock type, mineralogy and alterations

Origin	Common/Commercial Name	Colour	Structure – texture	Rock type	Mineralogy	Alterations
Pakistan*	Mansehra Granite	White to dark gray	Medium to Coarse grained porphyritic	Granite	Qz, K–F, Pl, Mu, Bi, Zr, Kaol, Ser, Op	Sericitization, Kaolinization
Pakistan [24, 31]	Ambela Granite	Greyish black to greenish black	Medium to coarse grained porphyritic	Alkali granite	A-F, Qz, Pl, Bi, traces of Ep, Tit, Amph, Chl, Zr, Ser	Sericitization
Spain [9]	Salvatierra	Light gray	Coarse grained porphyritic	Alkali granite	Qz, Pl, K–F, Bi, Tit, Zr, All, Chl, Kaol, Ser	Kaolinization, sericitization
Spain [9]	Rosa porrino	Pinkish	Coarse grained porphyritic	Alkali granite	Qz, Pl, K–F, Bi, Zr, Al, traces of Chl, Kaol, Ser	Mostly unaltered
India [9]	Multicolour	Light red–dark gray zones	Medium to coarse grained gneissic	Granite	Qz, Pl, K–F, Bi, Mu, Tit, Zr, Ap, Op, Kaol, Ser	Sericitization, Kaolinization
Finland [9]	Baltic brown	Dark brown	Coarse grained rapakivi	Granite	Qz, Pl, K–F, Bi, Amph, Zr, Ap, Op, Kaol	Kaolinization
Spain [9]	Gris perla	White to light gray	Coarse grained porphyritic	Granite	Qz, Pl, K–F, Bi, Amph, Tit, Zr, Ap, All, traces of Ep, Chl, Kaol, Ser	Almost unaltered
Norway [9]	Emerald	Black, iridescence	Coarse grained granitic	Quartz monzonite	A–F, Bi, Amph, Cpx, Ap, Op, traces of Kaol	Almost unaltered
Norway [9]	Marina pearl	Blue–gray iridescence	Coarse grained granitic	Quartz monzonite	A–F, Bi, Cpx, Ol, Zr, Ap, All, Ep, Op, traces of Kaol	Unaltered
South Africa [9]	Zimbabwe	Black	Medium grained granitic	Quartz monzodiorite	Qz, Pl, Opx, Cpx, Op	Unaltered
Brazil [9]	Yellow Cecilia	Yellow	Coarse grained porphyritic	Granite	Qz, Pl, K–F, Bi, Grt, Zr, Sil, traces of Kaol	Nearly unaltered
Brazil [9]	Napoleon	Yellow	Coarse grained porphyritic	Granite	Qz, Pl, K–F, Bi, Grt, Mu, Zr, Kaol, Ser	Kaolinization, sericitization
Finland [9]	Balmoral	Light red	Coarse grained granitic	Granite	Qz, Pl, K–F, Bi, Mu, Zr, Ap, Fl, Mz, traces of Ep, Chl, Kaol, Ser	Somewhat unaltered
South Africa [9]	African red	Dark red	Coarse grained granitic	Granite	Qz, Pl, K–F, Zr, Chl, Kaol, Ser	Strongly altered to kaolinite, sericite, chlorite
Brazil [9]	Topazio	Yellow to light brown	Coarse grained granitic	Granite	Qz, Pl, K–F, Bi, Grt, Zr, Op, Ac, Kaol, Ser	Marginally altered
Saudi Arabia [23]	Mount Arfat-Arabian Shield			Granodiorite	Qz, Pl, A-F, Bi, Ep, Ap, Tit	Sericitization, clinozoisite

Abbreviations: Qz = quartz, Pl = plagioclase, K-F = K-feldspar, A-F =alkali-feldspar, Bi = biotite, Mu = muscovite, Tit = titanite, Zr = zircon, Chl = chlorite, Kaol = kaolinite, Ser = sericite, Ap = apatite, Fl = fluorite,Amph = amphibole, Opx = orthopyroxene, Cpx = clinopyroxene, Ol = olivine, All = allanite, Mz = monazite, Ep = epidote, Ac = actinolithe, Sil = sillimanite, Op = opaque minerals

*Present Study, Rafiq and Jan 1988 [24], Arif et al. 2013 [30], Pavlidou et al. 2006 [9], Qureshi et al. 2012 [23].

samples of A3, A4 and A1 respectively as seen in Table 3. The specific activity of ^{40}K is higher than for ^{226}Ra and ^{232}Th because of its natural abundance in the earth's crust. The overall activity value of ^{226}Ra is lower than the permissible activity concentration of 40 Bq kg^{-1} for typical masonry materials [19]. However, the values of ^{232}Th and ^{40}K in Mansehra Granite are higher than the permissible limits of 40 and 400 Bqkg^{-1}respectively for masonry materials.

Average Specific activity for the four observable textural zones shows that Zone 1 has higher ^{226}Ra value (31.17 Bq kg^{-1}) while Zone 3 has higher ^{232}Th value (73.35 Bq kg^{-1})and Zone 4 has higher ^{40}K value (1056.67 Bq kg^{-1}) compared to other three Zones (Table 3). These specific activity values from each zone are different due to noticeable mineralogical variations (Table 1; Fig. 2; Fig. 4). Specific activity values of ^{40}K were found to be higher in high feldspar samples so it can be positively correlated with the relative content of feldspar [26]. Minerals hosting Uranium and Thorium could be responsible for higher activity concentration values of ^{226}Ra and ^{232}Th [27].

For comparison, the activity mass concentrations of ^{226}Ra, ^{232}Th and ^{40}K along with potential radioactive

Table 3: Comparison of Specific Activity values for ^{226}Ra, ^{232}Th and ^{40}K (Bq kg^{-1}) along with Outdoor Dose D_{out}, Indoor dose D_{in}, Annual Indoor effective dose E_{in}, Annual Outdoor effective dose E_{out} and Total Annual Dose (E) of Mansehra Granite, Pakistan with Universal limits.

Textural Zones	Sample Code	Specific Activity (Bq kg^{-1})			D_{out} nGy h^{-1}	D_{in} nGy h^{-1}	E_{out} mSv v^{-1}	E_{in} mSv y^{-1}	E (E_{out}+ E_{in}) mSv y^{-1}
		^{226}Ra	^{232}Th	^{40}K					
Zone 1	D4	38.37	83.24	1024.53	110.73	208.83	0.136	1.024	1.160
	D5	34.91	52.54	922.73	86.34	163.73	0.106	0.803	0.909
	E4	33.93	63.19	1090.15	99.30	187.94	0.122	0.922	1.044
	E5	17.98	28.70	984.11	66.68	126.84	0.082	0.622	0.704
	F4	32.19	63.80	976.77	94.13	177.91	0.115	0.873	0.988
	F5	29.64	63.77	1004.78	94.11	177.80	0.115	0.872	0.987
Zone 2	D1	24.62	26.30	1087.99	72.63	138.62	0.089	0.680	0.769
	D2	34.85	48.43	826.12	79.81	151.43	0.098	0.743	0.841
	D3	36.71	65.77	993.42	98.11	185.59	0.120	0.910	1.031
	E1	23.64	43.25	1036.11	80.25	152.21	0.098	0.747	0.845
	E2	26.68	76.46	963.96	98.71	185.77	0.121	0.911	1.032
	E3	23.46	38.85	960.40	74.35	141.15	0.091	0.692	0.783
	F1	31.8	51.50	1000.76	87.53	165.97	0.107	0.814	0.921
	F2	26.96	45.65	741.96	70.97	134.38	0.087	0.659	0.746
	F3	34.68	70.77	873.22	95.18	179.61	0.117	0.881	0.998
Zone 3	A4	25.72	87.01	197.65	72.68	135.19	0.089	0.663	0.752
	A5	27.37	77.40	1037.51	102.66	193.32	0.126	0.948	1.074
	B4	28.52	73.91	805.85	91.42	172.01	0.112	0.844	0.956
	C4	36.92	71.77	1160.15	108.78	205.73	0.133	1.009	1.142
	C5	31.33	56.64	700.56	77.90	147.17	0.096	0.722	0.817
Zone 4	A1	22.66	23.47	1227.82	75.85	144.90	0.093	0.711	0.804
	A2	22.91	34.74	948.53	71.12	135.18	0.087	0.663	0.750
	A3	50.91	55.62	366.47	72.40	137.34	0.089	0.674	0.762
	B1	17.56	24.27	1151.42	70.79	134.97	0.087	0.662	0.749
	B2	18.35	26.21	1215.83	75.01	142.98	0.092	0.701	0.793
	B3	22.88	43.99	1165.98	85.76	162.72	0.105	0.798	0.903
	C1	24.80	26.85	1141.12	75.26	143.64	0.092	0.705	0.797
	C2	27.72	39.97	1113.85	83.40	158.58	0.102	0.778	0.880
	C3	29.45	31.37	1179.02	81.72	155.92	0.100	0.765	0.865
Average Values	Overall Average	28.88	51.57	962.03	84.61	160.26	0.104	0.786	0.890
	Zone 1 Average	31.17	59.21	1000.51	91.88	173.84	0.113	0.853	0.965
	Zone 2 Average	29.27	51.89	942.66	84.17	159.41	0.103	0.782	0.885
	Zone 3 Average	29.97	73.35	780.34	90.69	170.68	0.111	0.837	0.948
	Zone 4 Average	26.36	34.05	1056.67	76.81	146.25	0.094	0.717	0.812
	Universal Limit	< 40 [19]	< 40 [19]	< 400 [19]	< 51 [19]	< 55[31]	< 1[29]	< 2[19]	< 1 [28]

minerals in Mansehra Granite with other granite varieties, used as building/decorative stones in world, [9, 23, 27] are presented in Table 4. The minimum values of ^{226}Ra occur in granite from Saudi Arabia, India and Brazil (11 Bq kg^{-1}) and maximum value (659 Bq kg^{-1}for Ambela Granite, Pakistan. Minimum and maximum values of ^{232}Th were found to be in granites of Saudi Arabia (29 Bq kg^{-1}) and Ambela granite, Pakistan (598 Bq kg^{-1}) respectively. Lowest Specific activity values of ^{40}K were found in granites of South Africa (Zimbabwe granite) (332 Bq kg^{-1}) and highest in Finland (Balmoral granite 1592 Bq kg^{-1}), respectively.

Table 4: Specific Activity values for ^{226}Ra, ^{232}Th and ^{40}K (Bq kg^{-1}) along with Annual effective dose E (mSv y^{-1}) values representing worldwide granite samples, in comparison with Mansehra Granite, Pakistan.

Origin	Common /Commercial Name	Potentially radioactive accessory minerals	Radionuclides (Bq kg^{-1})			Annual effective dose, E (mSv y^{-1})
			^{226}Ra	^{232}Th	^{40}K	
Pakistan*	Mansehra Granite	Zr, Ap	29	51	1218	0.9
Pakistan [27]	Ambela Granite	Ap, All, Zr, Ru	659	598	1203	5.1**
Spain [9]	Salvatierra	Tit, Zr, All	118	77	1320	1.4
Spain [9]	Rosa porrino	Zr, All	59	109	1420	1.4
Spain [9]	Blanco real	Zr, Ap, Mz	117	95	1233	1.4
Brazil [9]	Topazio	Zr, Hem, Ru	29	44	1327	0.8
Brazil [9]	Yellow Cecilia	Zr	19	30	1020	0.6
Spain [9]	Blanco crystal	Tit, Zr, Mz	163	91	1190	1.6
Brazil [9]	Napoleon	Zr	11	46	1200	0.7
Finland [9]	Balmoral	Zr, Ap, Fl, Mz,	170	354	1592	3.2
South Africa[9]	African red	Zr	80	121	1421	1.5
India [9]	Multicolour	Tit, Zr, Ap, Py, Hem	11	84	926	0.8
Finland [9]	Baltic brown	Zr, Ap, Py, Hem, Ilm	60	57	1350	1
Spain [9]	Gris perla	Tit, Zr, Ap, All	70	43	1340	1
Norway [9]	Emerald	Ap, Py, Hem	55	63	1053	1
Norway [9]	Marina pearl	Zr, Ap, Al, Py, Ilm	35	37	894	0.7
South Africa[9]	Zimbabwe	Py, Hem	20	32	332	0.4
Saudi Arabia [23]	Mount Arfat	Tit, Ap, Hem	11	29	664	0.045

Abbreviations: Tit = titanite, Zr = zircon,Fl = fluorite, Ap = apatite,Py = pyrite, Hem = hematite, Ilm = Ilmenite, All = allanite, Mz = monazite, Ru = rutile

*Present Study, Asghar et al. 2008 [27], Pavlidou et al. 2006 [9], Qureshi et al. 2012 [23],**Calculated for current study

3.3 Annual Effective Dose

3.3.1 Annual outdoor effective dose (E_{out})

E_{out} for a person working in the Mansehra Granite area was calculated using Eq. 3 and the results are given in Table 3. Average value of E_{out} comes out to be 0.104 mSv y^{-1} with a range of 0.082 to 0.136 mSv y^{-1}, which is below the limit of 1 mSv y^{-1} for the general public. For radiation workers the limit of Annual Outdoor Effective Dose (E_{out}) is 20 mSv y^{-1}. Average outdoor effective dose in Zone 1 is 0.113 mSv y^{-1} higher than other zones but within the limit proposed in UNSCEAR Report to the General Assembly, 2000 [19]. However the value is noticeable due to the composition of granite in Zones 1 and 3.

3.3.2 Annual indoor effective dose (E_{in})

Annual indoor effective dose (E_{in}) for Mansehra Granite was calculated using Eq. 5 and the results are given in Table 2. The average (E_{in}) value of 0.786 mSv y^{-1} with a range of 0.622 to 1.024 mSvy^{-1} is lower than the annual limit of 2 mSv y^{-1} [19] for the general public. So this hazard index falls in the safe limit. Average indoor effective dose values for Zones 1, 2, 3 and 4 are 0.853, 0.782, 0.837 and 0.717 mSv y^{-1} respectively. Compared to other zones, Zones 1 and 3 have a higher average values of E_{in} (Table 3).

Total annual effective dose (E) was calculated by adding indoor and outdoor effective dose values and average value was found to be 0.890 mSv y^{-1} with a range of 0.704 to 1.160 mSv y^{-1}.This is lower than the annual limit of 1 mSv y^{-1} for general public [19] with the exception of some samples listed in Table 3. From Table 3 it can be seen that the average values of total effective dose in four textural zones were found to be distributed in such a way that Zones 1 and 3 have higher values (0.965 mSv y^{-1} and 0.948 mSv y-1 respectively) as compared to Zones 2 and 4 (0.885 mSv y^{-1} and 0.812 mSv y^{-1} respectively). Average total effective dose values of respective zones accurately demonstrate the impact of mineralogical variations in granite on the dose rates. Despite high specific activity values of ^{40}K, results show low values of total effective dose in Zone 4, which could be clarified by its least contribution factor as compared to ^{226}Ra and ^{232}Th as shown in Eqs. 2 and 4. Granites from Pakistan (Ambela), Finland, Spain and South Africa (African red) possessed annual effective doses higher than 1 mSv y^{-1} (Table 4). Average annual effective dose of Mansehra granite was calculated to be 0.9 mSv y^{-1}. Accessory minerals that were found to be enhancing annual effective dose values in granites from Spain and South Africa were zircon, allanite and titanite. Accessory minerals in Ambela granite (Pakistan) were apatite, allanite, zircon and rutile. Zircon and apatite were also

found in minor quantities in Mansehra granite, Pakistan. These minerals act as a host for radioactive nuclides which occur in the form of U or Th compounds [5]. In Table 4 the specific activity, annual effective dose and potential radioactive minerals present in renowned granites around the world are compared.

4. Conclusion

Results of this study suggest that the presence of uranium and thorium bearing minerals in Zones 1 and 3 are responsible for higher activity concentration and dose rates observed in these Zones. Observable megascopic and microscopic study in Zones 1 and 3 depict noticeable variations in primary minerals; microcline, biotite, plagioclase and accessory minerals like zircon, apatite, tourmaline, magnetite etc. as compared to Zones 2 and 4. This imparts higher dose rates and activity concentration to the former Zones. Overall, radioactivity in Mansehra Granite falls within safe limit for most of the radiological indices [19, 31, 32]. Specific activity of isotopes of Radium, Thorium and Potassium is controlled by variations in mineralogical composition.

Calculations of annual effective dose rates yielded values of hazard indices, which are below their limiting values defined by UNSCEAR. Annual effective dose rates are found to be higher in Zones 1 and 3 as compared to other Zones. Thus precautionary measures should be taken when Granite is excavated from these Zones. Use of Mansehra Granite in construction and decorating industry like tiles, slabs and countertops is safe from radiological hazard point of view. However, it is suggested to limit the use of granite to outdoors and architectural design of buildings should incorporate proper ventilation systems to minimize radiation risk.

Acknowledgement

Authors would like acknowledge to Radiation Physics Lab, Physics Department, COMSATS Islamabad, Pakistan for providing instrumentation and support for this research work. Authors are also grateful to Mr. Aosaf Hassan (Quaid-i-Azam University) and Mr. Muhammad Nasir (Geological Survey of Pakistan) for their help in petrographic study. Authors are also grateful to esteemed reviewers for their contribution in improving this document.

References

[1] TF Gesell and HM. Prichard, “The technologically enhanced natural radiation environment”, Health Physics, vol. 28, pp. 361-366, 1975.

[2] ICRP. ICRP Publication 65, Ann. ICRP 23 (2), 1994.

[3] MIA, “Truth about granite and radon exhalation”, Marble Institute of America, Cleveland, Ohio, 2007.

[4] B. Mason and C. Moore, “Principles of geochemistry”, Fourth Ed. Wiley, New York, 1982.

[5] EW. Heinrich, “Mineralogy and geology of radioactive raw materials”, McGraw-Hill Book Company, New York, 1958.

[6] M. Tzortzis and H. Tsertos, “Determination of thorium, uranium and potassium elemental concentrations in surface soils in Cyprus”, Journal of Environmental Radioactivity, vol. 77, pp. 325-338, 2004.

[7] I. Basham, B. Beddoe-Stephens, T. Ball and UM. Michie, “Uranium-bearing accessory minerals and granite fertility: 1. Methods of identification and evaluation”, Proceedings of the Symposium on Uranium Exploration Methods, OECD, Paris, pp. 385-397, 1982.

[8] S. Tjokrokardono, “Radioactive Minerals Species of Maisah Tertiary Granite, South Sulawesi”, Atom Indonesia, vol. 26, pp. 25-39, 1995.

[9] S. Pavlidou, A. Koroneos, C. Papastefanou, G. Christofides, S. Stoulos and M. Vavelides, “Natural radioactivity of granites used as building materials”, J. Environ. Radioactiv., vol. 89, p. 48-60, 2006.

[10] Y. Örgün, N. Altınsoy, A. Gültekin, G. Karahan and N. Celebi, “Natural radioactivity levels in granitic plutons and groundwaters in Southeast part of Eskisehir, Turkey”, App. Radiat. and Isotop., vol. 63, pp. 267-275, 2005.

[11] J.A. Calkins, T.W. Offield, S. Abdullah and ST. Ali, “Geology of the southern Himalaya in Hazara, Pakistan, and adjacent areas”, Geological Survey Professional Paper, US Government Printing Office, vol. 716-C, pp. 1–29, 1975.

[12] F.A. Shams, “Geology of the Mansehra-Amb State Area, North-Western Pakistan”, Geological Bulletin, Punjab University, Lahore, vol. 8, pp. 1-32, 1969.

[13] M. Arif, A. Mulk, M. Tariq and S. Majid, “Petrography and mechanical properties of the Mansehra granite, Hazara, Pakistan”, Geological Bulletin, University of Peshawar, vol. 32, pp. 41-49, 1999.

[14] AA. Qureshi, IAK. Jadoon, AA. Wajid, A. Attique, A. Masood, M. Anees, S. Manzoor, A. Waheed and A. Tubassam, "Study of natural radioactivity in Mansehra granite, Pakistan: environmental concerns." Radiation protection dosimetry, vol. 4, pp. 466-478, 2014.

[15] Geological Survey of Pakistan, “Geological map of Pakistan 1:1,000,000”, 1993.

[16] CM. Lederer, JM. Hollander and I. Perlman, “Table of Isotopes”, 6th ed. John Wiley & Sons, New York, 1968.

[17] P. Hayambu, M. B. Zaman, N. C. H. Lubaba, S. S. Munsanje and D Muleya, “Natural radioactivity in Zambian building materials collected from Lusaka”, J. Radioanal. Nucl. Chemi., vol. 99 3, pp. 229-238, 1995

[18] IAEA Technical Report 309, “Construction and use of calibration facilities for radiometric field equipment, Subject-Uranium Geology, Exploration and Mining, 1989.

[19] UNSCEAR, Sources and Effects of Ionizing Radiation, United Nations Scientific Committee on the Effects of Atomic Radiation (UNSCEAR), Report to the General Assembly, with Scientific Annexes, p. 116, 2000.

[20] European Commission Radiological protection principles concerning the natural radioactivity of building materials. Radiation Protection Report RP-112 European Commission, Luxembourg, p.8, 1999.

[21] M. Naeem, P. Khalid and AW. Anwar, “Construction material prospects of granitic and associated rocks of Mansehra area, NW Himalaya, Pakistan”, Acta Geodaeticaet Geophysica, vol. 50, no. 3, pp. 307-319, 2015.

[22] K. Butt and Z. Shah, “Discovery of blue beryl from Ilum granite and its implications on the genesis of emerald mineralization in Swat district”, Geological Bulletin University of Peshawar, vol. 18, pp. 75-81, 1985.

[23] AA. Qureshi, A. Sultan, A. Rashid, M. Ali, A. Waheed, S. Manzoor, M. A. Baloch, S. Batool, and H. A. Khan, "Geological and radiological studies of the Mount Arafat, Mekkah, Saudi

Arabia", Journal of Radioanalytical and Nuclear Chemistry, vol. 3, pp. 955-963, 2012.

[24] M. Rafiq and MQ. Jan, "Petrography of the Ambela granitic complex, NW Pakistan", Geological Bulletin University of Peshawar, vol. 21, pp. 27-48, 1988.

[25] P. Le Fort, F. Debon and J. Sonet, "The Lesser Himalayan cordierite granite belt. Typology and age of the Pluton of Manserah (Pakistan)", Proceedings of the International Committee on Geodynamics Group 6 Meeting: Geological Bulletin, University of Peshawar, Secial Issue, pp 51-61, 1980.

[26] J. Guillén, J. Tejado, A. Baeza, J. Corbacho and J. Muñoz, "Assessment of radiological hazard of commercial granites from Extremadura (Spain)", Journal of environmental radioactivity, vol. 132, p. 81-88, 2014.

[27] M. Asghar, M. Tufail, J. Sabiha, A. Abid and M. Waqas, "Radiological implications of granite of northern Pakistan", J. Radiol. Prot., vol. 28, p. 387-399, 2008.

[28] ICRP. ICRP Publication 60, Ann. ICRP 21, 1-3, 1991.

[29] ICRP. ICRP Publication 103, Ann. ICRP 37, 2-4, 2007

[30] M. Arif, S. Bukhari, N Muhammad and M. Sajid, "Petrography and Physicomechanical Properties of Rocks from the Ambela Granitic Complex, NW Pakistan", The Scientific World Journal, vol. 2013, pp. 1-8, 2013, doi:10.1155/2013/349381.

[31] UNSCEAR, Sources and Effects of Ionising Radiation. United Nations Scientific Committee on the Effects of Atomic Radiation (UNSCEAR), Report to the General Assembly, with Scientific Annexes, 1993.

[32] UNSCEAR, Sources, Effects and Risks of Ionizing Radiation. United Nations, New York, 1998.